Topological Jamming of Spontaneously Knotted Polyelectrolyte Chains Driven Through a Nanopore

A. Rosa,[1,*] M. Di Ventra,[2] and C. Micheletti[1,3,†]

[1]SISSA—Scuola Internazionale Superiore di Studi Avanzati, Via Bonomea 265, 34136 Trieste, Italy
[2]Department of Physics, University of California, San Diego, La Jolla, California 92093-0319, USA
[3]CNR-IOM Democritos, Via Bonomea 265, 34136 Trieste, Italy

(Received 12 April 2012; published 12 September 2012)

The advent of solid state nanodevices allows for interrogating the physicochemical properties of a polyelectrolyte chain by electrophoretically driving it through a nanopore. Salient dynamical aspects of the translocation process have been recently characterized by theoretical and computational studies of model polymer chains free from self-entanglement. However, sufficiently long equilibrated chains are necessarily knotted. The impact of such topological ''defects'' on the translocation process is largely unexplored, and is addressed in this Letter. By using Brownian dynamics simulations on a coarse-grained polyelectrolyte model we show that knots, despite being trapped at the pore entrance, do not *per se* cause the translocation process to jam. Rather, knots introduce an effective friction that increases with the applied force, and practically halts the translocation above a threshold force. The predicted dynamical crossover, which is experimentally verifiable, ought to be relevant in applicative contexts, such as DNA nanopore sequencing.

DOI: 10.1103/PhysRevLett.109.118301 PACS numbers: 36.20.Ey, 02.10.Kn, 82.35.Lr, 87.15.A−

Nanopores, namely holes of nanoscale dimensions carved out of biological or solid-state membranes, are increasingly becoming an important tool to probe chemical and physical properties of polymers [1–6]. For instance, polyelectrolytes, such as DNA, can be electrophoretically translocated through a pore and their chemical composition can be inferred either by the ionic current blockaded by the DNA strand [7], or from the electrical current measured perpendicular to the DNA backbone [8]. These approaches are being actively investigated because they hold great promise for fast and low-cost DNA sequencing.

However, one of the issues that has received much less attention is related to possible limitations arising from the maximum length of the polymer that can be electrophoretically translocated through a nanopore without obstruction from the inevitable chain self-entanglement (knots). In fact, it is well known that the incidence of knots increases rapidly with the chain contour length and, in turn, can affect kinetic, mechanical and equilibrium properties of sufficiently long (bio-)polymers both in bulk and in confining geometries [9–20]. A knot in the polymer chain is then an unwanted potential obstruction to its translocation through a pore; much like the knot we customarily make at the end of a sewing thread to prevent it from ''translocating'' through a threaded piece of cloth.

Motivated by these observations, in this Letter we set out to investigate theoretically and numerically the dynamics of pore translocation of chains whose contour length exceeds by orders of magnitude their persistence length. On the one hand, this allows us to push to unprecedented contour lengths the assessment of the validity of previously suggested dynamical scaling relationships for the translocation process of unknotted chains (see, e.g., Refs. [21–27]). On the other hand, we can clarify the impact of spontaneous knotting on the driven translocation of biopolymers. This avenue appears to be largely unexplored except for the recent protein-related investigation of Huang and Makarov [15].

In particular, we show that knots do not *per se* cause the translocation process to halt. More precisely, they are found to act as pluglike obstructions of the pore only if a threshold driving force is exceeded. Based on this result it is expected that accounting for the topology-dependent dynamical crossover ought to be important for applications that employ nanopores, such as the detection and sequencing of DNA filaments [1,2,28].

We consider a model polyelectrolyte chain that is electrophoretically driven through a pore embedded in the slab separating the *cis* and *trans* semispaces [1]. For definiteness, the salient physical properties of the (otherwise general) model system are set to match those of 15 μm-long ssDNA filaments in a solution with 0.1 M monovalent salt and translocated through an artificial nanopore, see Fig. 1. Unless otherwise stated, the nominal slab thickness and effective pore diameter were set respectively equal to 10 nm and 1.76 nm [29], consistent with the typical geometries of solid state nanopores (which are longer than biological ones [28]) with or without functionalized walls [1,2].

The polyelectrolyte chain consists of $N = 15000$ beads, with diameter equal to the nominal ssDNA thickness, $\sigma = 1$ nm. Because the monovalent counterions reduce the phosphates electrostatic charge by $\sim$50% [30] the effective charge of the beads, each spanning three nucleotides,

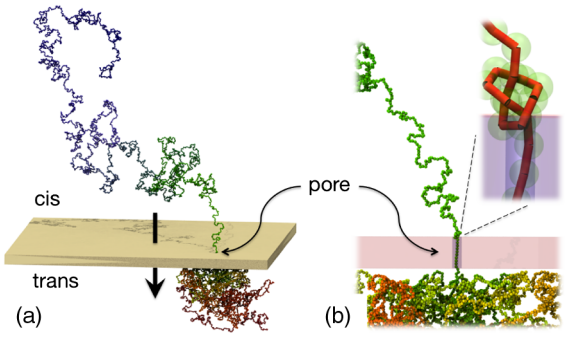

FIG. 1 (color online). (a) Snapshot of a model polyelectrolyte chain consisting of 15 000 beads driven electrophoretically through a nanopore. The arrow indicates the translocation direction. (b) Cut-through view of the pore region for configuration in panel (a). The chain backbone, with a tightened trefoil knot at the pore entrance, is highlighted in the inset.

is set equal to $q = -1.5e$. The chain potential energy is accordingly given by:

$$\mathcal{H} = \sum_{i=1}^{N}\Big\{U_{\mathrm{FENE}}(d_{i,i+1}) + \frac{1}{2}\sum_{j=1,j\neq i}^{N}[U_{\mathrm{LJ}}(d_{i,j}) + U_{\mathrm{DH}}(d_{i,j})]\Big\},$$

where $d_{i,j}$ is the distance of monomers i and j, and the three terms, which enforce respectively the chain connectivity constraint (U_{FENE}), the pairwise Lennard-Jones interaction (U_{LJ}), and Debye-Hueckel (U_{DH}) repulsion have the form:

$$U_{\mathrm{FENE}}(d) = \begin{cases} -150\kappa_B T\left(\frac{R_0}{\sigma}\right)^2 \ln\left[1-\left(\frac{d}{R_0}\right)^2\right], & d \le R_0, \\ 0, & d > R_0 \end{cases}$$

$$U_{\mathrm{LJ}}(d) = \begin{cases} 4\kappa_B T\epsilon_{i,j}\left[\left(\frac{\sigma}{d}\right)^{12} - \left(\frac{\sigma}{d}\right)^{6} + 1/4\right], & d \le \sigma 2^{1/6}, \\ 0, & d > \sigma 2^{1/6} \end{cases}$$

$$U_{\mathrm{DH}}(d) = \frac{q^2 e^{-d/\lambda_{\mathrm{DH}}}}{\varepsilon d},$$

where $R_0 = 1.5\sigma$, κ_B is the Boltzmann constant, $T = 300\,\mathrm{K}$, $\varepsilon = 80$ is the water dielectric constant, $\lambda_{\mathrm{DH}} = 0.9$ nm is the Debye screening length, and $\epsilon_{i,j}$ is equal to 1 if $|i-j|=1$, and 10 otherwise.

A Monte Carlo scheme, employing unrestricted, nontopology-preserving local and global moves [10,31], was first used to generate an equilibrated set of conformations for flexible self-avoiding chains of $N = 15000$ beads in bulk. The degree and type of entanglement of the filaments was established using the minimally-interfering closure scheme [32,33].

We found that the fraction of chains that were knotted in equilibrium was about 2%. Such incidence, when normalized by contour length, is compatible with that previously reported for shorter flexible open chains [34]. The knots spanned, on average, about 10% of the chain and in more than 90% of the cases they corresponded to the simplest knot type: the trefoil or 3_1 knot [see example in the inset of Fig. 1(b)].

Since the main focus of the Letter concerns the impact of chain topology on the translocation dynamics, we neglect here the otherwise important issue of how a chain in the bulk approaches the pore and enters it [35]. Accordingly, we extracted from the equilibrated ensemble several uncorrelated knotted and unknotted chains, for which a rigid global translation or rotation could bring one of the ends at the pore entrance while the chain remainder stays in the *cis* semispace.

The beads inside the pore are driven through it by a constant force whose magnitude, f, typically falls in the 4–40 pN range. Assuming that the electro-osmotic screening inside the channel [6,36] reduces by ~50% the charge density of ssDNA, these forces correspond to a uniform electric field of 0.15–1.5 V per 10 nm acting on *each* bead. The translocation dynamics of the polyelectrolyte chain is integrated numerically using the fixed-volume and constant-temperature molecular dynamics simulation scheme implemented in the LAMMPS package [37]. As in other coarse-grained approaches, no explicit hydrodynamic treatment is introduced [38]. A typical instantaneous configuration of the translocating chain is shown in Fig. 1.

Unknotted chain dynamics.—Fig. 2(a) illustrates the translocation dynamics for various pulling forces after averaging over an ensemble of 20 *unknotted* chains. The dependence of the dynamics on the initial arrangement of

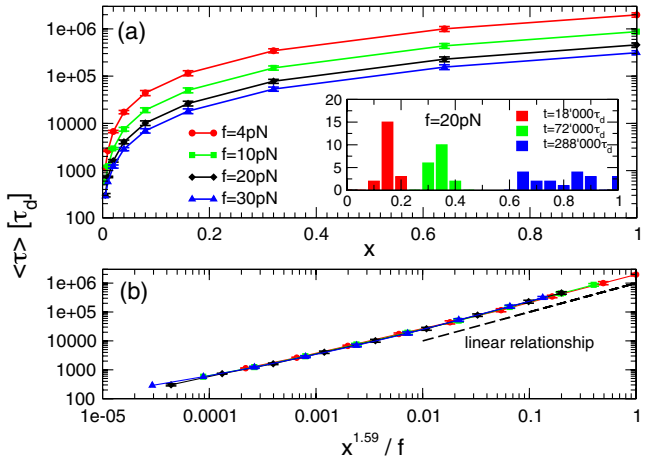

FIG. 2 (color online). (a) Average time, $\langle\tau\rangle$, required to translocate a fraction x of an unknotted chain at various driving forces, f. The average is taken over 20 uncorrelated unknotted conformations. Inset: statistical distribution of x at three different times and $f = 20$ pN. Because the process time scale falls in the overdamped regime, time is expressed in units of the nominal monomer self-diffusion time: $\tau_d = \pi\eta\sigma^3/2\kappa_B T$. For water viscosity, $\eta = 1$ cP, $\tau_d \sim 0.5$ ns [42]. (b) Collapse of the data points in panel (a) using the theoretical dynamical scaling, see text.

the chain reflects in the fact that the distribution of the translocated chain fraction, x, has a spread that increases with time, see inset in Fig. 2(a). Notwithstanding this feature, the average asymptotic translocation times appear to follow closely [see Fig. 2(b)] the dynamical scaling relationship predicted theoretically [21–23], $\langle\tau\rangle \propto x^{1+\nu}/f$ where $\nu = 0.59$ is the metric exponent of a self-avoiding polymer [39].

It should be noted that this scaling relationship, which was first formulated using dimensional and heuristic arguments [21–23], was more recently shown to hold only for asymptotically long chains [27]. In fact, the nonequilibrium process that governs the propagation of the tensile disturbance along the chain is sensitive to finite chain effects [27]. The collapse of the data points in Fig. 2(b) clarifies that the theoretically predicted asymptotic scaling relationship holds satisfactorily for chains of $N = 15000$ beads with the considered driving protocol.

Knotted chain dynamics.—Compared to the unknotted case, the translocation dynamics of knotted chains has a dramatic, nonmonotonic dependence on the driving force. This is illustrated in Fig. 3 for one particular trefoil-knotted configuration where the knot occupies the midportion of the chain and spans about 10% of the chain. It is seen that at the smallest driving force, the chain translocation is well consistent with the average dynamics of unknotted chains. At higher forces, however, the standard dynamic scaling is satisfied only up to when about 50% of the chain is translocated, after which a noticeable slowing down of the process ensues. Notice that at the highest force, the translocation process appears to be practically halted.

This *dynamical crossover* is understood by monitoring the instantaneous position and size of the knot along the chain. The data for $f = 20$ pN are shown in Fig. 4. It is seen that the knot position along the chain is unperturbed until it is reached by the propagating pulling front. At this stage, the progressive dragging of the chain through the pore causes the knot to tighten. Notice that, because the sequence index of the knot distal end remains about constant in time, the knot tightening process consists of the removal of the "slack" from the end that is nearest to the pore. After this stage, the tightened knot is localized at the pore entrance and the translocation proceeds by chain reptation through the knot "defect." These results illustrate the remarkable impact that nontrivial *spontaneous entanglement* of long polymer chains has on the translocation dynamics as a function of the pulling force.

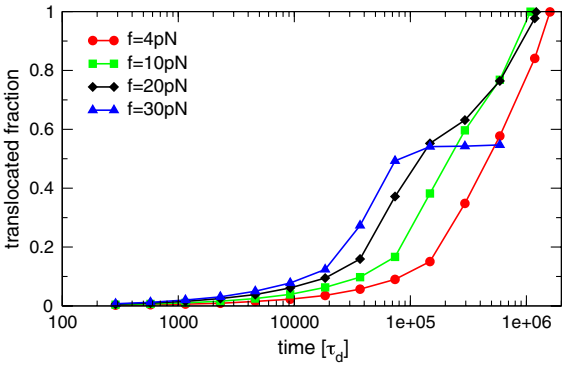

FIG. 3 (color online). Translocation kinetics of a specific trefoil-knotted chain at various driving forces. The time behavior for knotted chains with different initial configurations is qualitatively similar, with chains being halted at the same force, $f = 30$ pN.

To quantify in the most transparent way the topology-dependent aspect of the effect, and separate it from the one associated to the chain geometry we have extended our analysis in two complementary directions. First, by comparing the dynamics of chains with same geometry, but different topology near the pore entrance. Secondly, by suitably averaging the translocation dynamics over chains with different geometry but same knot topology.

For the first analysis, immediately after the knot is tightened at the pore entrance, one can locally perturb the chain geometry at the pore so as to untie the knot, while leaving unaltered the coordinates of all other parts of the chains, see Fig. 5. Next, by following both the dynamical evolution of the knotted and unknotted versions of the chain (with the same initial velocities for both simulations) it is possible to compare the net effect of the localized knot defect on the chain translocation dynamics. The results are shown in Fig. 5 and aptly illustrate that the slowing down of the translocation process is ascribable to the presence of the localized knot at the pore entrance.

A quantitative assessment of the topology-dependent hindrance can be made by comparing the average translocation times of unknotted chains [see Fig. 2(a)] and of knotted ones where the knot is initially close to the pore entrance. Specifically, we considered chains where the

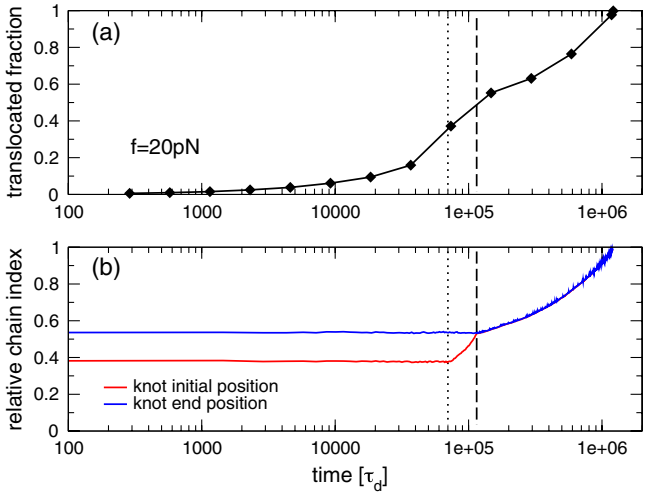

FIG. 4 (color online). Dynamical evolution (a) of the translocated chain fraction and (b) of the relative knot location along the chain for the same translocation run at $f = 20$ pN shown in Fig. 3. At time $t \sim 7 \times 10^4 \tau_d$ (dotted line) the propagating pulling front reaches the knot which progressively tightens until it reaches the pore at $t \approx 1.2 \times 10^5 \tau_d$ (dashed line).

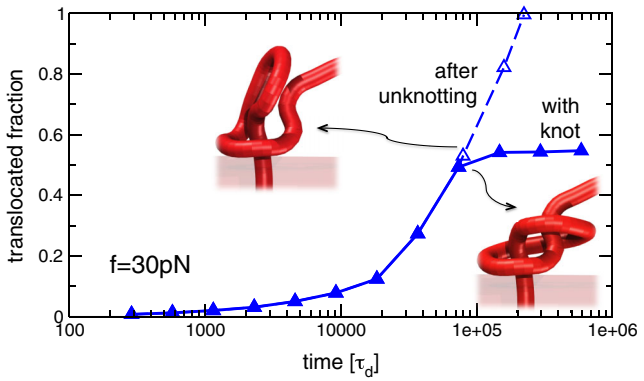

FIG. 5 (color online). Dependence of the translocation dynamics on the chain topology. After unknotting the chain by the shown local modification of the chain at the pore entrance the translocation velocity is dramatically enhanced. For clarity, here and in Fig. 6 the chain centerline is rendered as a continuous tube with diameter smaller than σ.

knot was located within the first 10%–20% of the chain, and for which the knot tightening and trapping occurs within a time span that is typically less than 5% of the full translocation process. We computed the effective friction coefficient, γ_{knot}, of these knot-dominated processes and found that it has a dramatic dependence on f. This contrasts with the unentangled case where γ_0 is practically force independent, as testified by the collapse of the data in Fig. 2. The effect is illustrated in Fig. 6. Notice that at the lowest pulling force, $f = 4$ pN, where a fairly tight knot (spanning 27 monomers on average) is trapped at the pore entrance, γ_{knot} is statistically compatible with γ_0.

We therefore conclude that knot localization at the pore entrance is not *per se* an impediment for translocation. It becomes so only when sufficiently high pulling forces

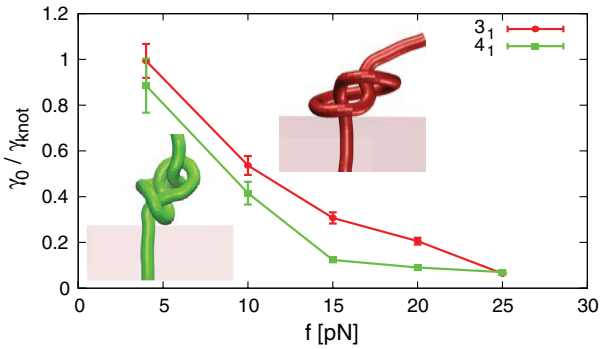

FIG. 6 (color online). Force dependence of the normalized inverse friction coefficient, $\gamma_0/\gamma_{\mathrm{knot}}$ for chains hosting 3_1 knots and 4_1 knots. At each force, γ_0 is defined as $\gamma_0 \equiv \langle \tau_t \rangle f/\sigma$, where $\langle \tau_t \rangle$ is the average time required by unknotted chains to fully translocate. An analogous definition is used to compute γ_{knot} for 3_1- and 4_1-knotted chains. Averages are taken over 20 configurations for the unknotted case and five configurations for each nontrivial topology. The bars indicate the standard error of the mean.

cause the chain beads to interact very tightly, resulting in a rapidly increasing effective friction. Consistent with the dynamics in Figs. 4 and 5, the trend in Fig. 6 indicates that the translocation process is practically halted at $f \sim 30$ pN.

It is interesting to notice that the observed impact of topology on dynamics differs from the case of knotted chains that are passively ejected out of a small spherical cavity [40,41]. In such systems, knots—even when tight—reduce the ejection speed by only a factor of 2–3 [40], possibly due to the relatively small magnitude of the force driving the spontaneous ejection.

Yet, in accord to available numerical results for knot-controlled DNA ejection [40] and protein translocation dynamics [15], we do observe that at moderate driving forces the dynamical hindrance is appreciably higher for knots that are more complex (and rarer) than trefoils. In fact, as it is shown in Fig. 6 the average inverse friction coefficient of 4_1-knotted chains is noticeably smaller than of 3_1-knotted ones. Forces in the 30–40 pN range are nevertheless sufficient to halt the translocation process of 4_1-knotted configurations and of 5_1- and 5_2-knotted ones [29].

Finally, we stress that the results presented here ought to be relevant in applicative contexts, such as genomic nanopore sequencing where the high-throughput demand pushes towards interrogating longer and longer uninterrupted DNA filaments at pulling forces comparable to those considered in this work [1,2]. The high-throughput condition inevitably leads to significant chain self-entanglement, while high pulling forces may cause tight knots to halt the translocation process. It should also be pointed out that in actual ssDNA chains the latter effect will expectedly be more severe than in our model system because of the ramified character of the molecule, and base-pairing effects. An analogous enhancement is expected for standard, nonfunctionalized nanopores which are typically narrower than the pore considered here. Wider pores can still jam chains with all the previously mentioned knotted topology, as long as the pore section is smaller than what is needed to accommodate three chain strands. In fact, at such a channel width, which is about 2.3 nm for our system, tight trefoil knots are sufficiently slender to slip through the pore, while more complex knots remain trapped and jammed at the pore entrance [29]. Since it would be challenging to resolve the sequence of a tightly knotted ssDNA portion slipping through the channel, it is suggested that pores of width smaller than 2.3 nm ought to be used to sequence long (and hence entangled) ssDNA filaments.

Since, the predicted force-dependent topological jamming is experimentally verifiable, we hope that the present investigation will motivate further studies aimed at quantifying this effect.

We acknowledge support from the Italian Ministry of Education and the National Human Genome Research Institute of NIH.

*anrosa@sissa.it
†michelet@sissa.it

[1] M. Zwolak and M. Di Ventra, Rev. Mod. Phys. **80**, 141 (2008).
[2] D. Branton *et al.*, Nat. Biotechnol. **26**, 1146 (2008).
[3] W. Reisner, K. J. Morton, R. Riehn, Y. M. Wang, Z. Yu, M. Rosen, J. C. Sturm, S. Y. Chou, E. Frey, and R. H. Austin, Phys. Rev. Lett. **94**, 196101 (2005).
[4] A. J. Storm, C. Storm, J. Chen, H. Zandbergen, J.-F. Joanny, and C. Dekker, Nano Lett. **5**, 1193 (2005).
[5] B. Luan and A. Aksimentiev, Soft Matter **6**, 243 (2010).
[6] S. van Dorp, U. F. Keyser, N. H. Dekker, C. Dekker, and S. G. Lemay, Nature Phys. **5**, 347 (2009).
[7] J. J. Kasianowicz, E. Brandin, D. Branton, and D. W. Deamer, Proc. Natl. Acad. Sci. U.S.A. **93**, 13770 (1996).
[8] J. Lagerqvist, M. Zwolak, and M. Di Ventra, Nano Lett. **6**, 779 (2006).
[9] E. Ercolini, F. Valle, J. Adamcik, G. Witz, R. Metzler, P. De Los Rios, J. Roca, and G. Dietler, Phys. Rev. Lett. **98**, 058102 (2007).
[10] C. Micheletti, D. Marenduzzo, and E. Orlandini, Phys. Rep. **504**, 1 (2011).
[11] V. V. Rybenkov, N. R. Cozzarelli, and A. V. Vologodskii, Proc. Natl. Acad. Sci. U.S.A. **90**, 5307 (1993).
[12] A. M. Saitta, P. D. Soper, E. Wasserman, and M. L. Klein, Nature (London) **399**, 46 (1999).
[13] X. R. Bao, H. J. Lee, and S. R. Quake, Phys. Rev. Lett. **91**, 265506 (2003).
[14] J. I. Sulkowska, P. Sulkowski, P. Szymczak, and M. Cieplak, Phys. Rev. Lett. **100**, 058106 (2008).
[15] L. Huang and D. E. Makarov, J. Chem. Phys. **129**, 121107 (2008).
[16] J. Arsuaga, M. Vázquez, S. Trigueros, D. W. Sumners, and J. Roca, Proc. Natl. Acad. Sci. U.S.A. **99**, 5373 (2002).
[17] A. Y. Grosberg and Y. Rabin, Phys. Rev. Lett. **99**, 217801 (2007).
[18] J. Tang, N. Dub, and P. S. Doyle, Proc. Natl. Acad. Sci. U.S.A. **108**, 16153 (2011).
[19] N.-K. Lee, C. F. Abrams, A. Johner, and S. Obukhov, Phys. Rev. Lett. **90**, 225504 (2003).
[20] D. Meluzzi, D. E. Smith, and G. Arya, Annu. Rev. Biophys. **39**, 349 (2010).
[21] Y. Kantor and M. Kardar, Phys. Rev. E **69**, 021806 (2004).
[22] C. Chatelain, Y. Kantor, and M. Kardar, Phys. Rev. E **78**, 021129 (2008).
[23] A. Y. Grosberg, S. Nechaev, M. Tamm, and O. Vasilyev, Phys. Rev. Lett. **96**, 228105 (2006).
[24] T. Sakaue, Phys. Rev. E **76**, 021803 (2007).
[25] T. Sakaue and E. Raphaël, Macromolecules **39**, 2621 (2006).
[26] C. Forrey and M. Muthukumar, J. Chem. Phys. **127**, 015102 (2007).
[27] T. Ikonen, A. Bhattacharya, T. Ala-Nissila, and W. Sung, Phys. Rev. E **85**, 051803 (2012).
[28] I. M. Derrington, T. Z. Butler, M. D. Collins, E. Manrao, M. Pavlenok, M. Niederweis, and J. H. Gundlach, Proc. Natl. Acad. Sci. U.S.A. **107**, 16060 (2010).
[29] See Supplemental Material at http://link.aps.org/supplemental/10.1103/PhysRevLett.109.118301 for translocation examples with various knot types and pore sizes.
[30] C. Maffeo, R. Schöpflin, H. Brutzer, R. Stehr, A. Aksimentiev, G. Wedemann, and R. Seidel, Phys. Rev. Lett. **105**, 158101 (2010).
[31] N. Madras and A. D. Sokal, J. Stat. Phys. **50**, 109 (1988).
[32] L. Tubiana, E. Orlandini, and C. Micheletti, Prog. Theor. Phys. **191**, 192 (2011).
[33] L. Tubiana, E. Orlandini, and C. Micheletti, Phys. Rev. Lett. **107**, 188302 (2011).
[34] P. Virnau, Y. Kantor, and M. Kardar, J. Am. Chem. Soc. **127**, 15102 (2005).
[35] M. Muthukumar, J. Chem. Phys. **132**, 195101 (2010).
[36] B. Luan and A. Aksimentiev, Phys. Rev. E **78**, 021912 (2008).
[37] S. Plimpton, J. Comput. Phys. **117**, 1 (1995).
[38] I. Ali and J. M. Yeomans, J. Chem. Phys. **123**, 234903 (2005).
[39] M. Doi and S. F. Edwards, *The Theory of Polymer Dynamics* (Oxford University Press, New York, 1986).
[40] R. Matthews, A. A. Louis, and J. M. Yeomans, Phys. Rev. Lett. **102**, 088101 (2009).
[41] D. Marenduzzo, E. Orlandini, A. Stasiak, D. Sumners, L. Tubiana, and C. Micheletti, Proc. Natl. Acad. Sci. U.S.A. **106**, 22269 (2009).
[42] K. Kremer and G. S. Grest, J. Chem. Phys. **92**, 5057 (1990).